Phys. Chem. Chem. Phys. 4,11 (2002) 2398-2408.

# UV/Vis/near-IR spectroscopic characteristics of $H_{4-x}Cs_xPVMo_{11}O_{40}$ (x = 0, 2) catalyst under different temperatures and gas atmospheres

J. Melsheimer*[1], J. Kröhnert[1], R. Ahmad[1], S. Klokishner[2], F. C. Jentoft[1], G. Mestl[1]and R. Schlögl[1]

[1] Department of Inorganic Chemistry, Fritz-Haber-Institute of the MPG, Faradayweg 4-6, 14195 Berlin, Germany
[2]State University of Moldova, Mateevich str.60, 2009 Kishinev, Moldova,

* Corresponding author: e-mail jm@fhi-berlin.mpg.de,

**Abstract**

In order to understand the transformations of the Keggin-type $H_{4-x}Cs_xPVMo_{11}$ (x=0,2) compounds with rising temperature over long time stream of different gas athmospheres, in situ UV/Vis/near-IR spectroscopic studies were carried out. Diffuse reflectance spectra were recorded using an improved spectrometer and a suitable microreactor. Visible and near-IR peak intensities, peak positions and the band gap energies were determined from apparent absorption spectra. Propene, iso-propanol, water and the oxidation products were analyzed by GC. The experimental observed blue shift of the visible absorption band in the range of crystal water loss and the increase of the near-IR absorption were explained on the basis of quantum-mechanical calculations of the shapes and positions of the charge transfer and d-d bands arising from $Mo^{5+}$-$Mo^{6+}$ and $V^{4+}$-$Mo^{6+}$ pairs in intact and ill-defined fragments of the Keggin structure. It was concluded that with removal of crystal water during the action of He, He/$H_2O$, propene, $O_2$/propene and increasing temperature reduced species with protons located at the bridging oxygens promote a blue shift of the visible band, while a large number of ill-defined species form the near-IR part of the spectra in the temperature range 326 - 600 K.

## 1. Introduction

Cs salts of vanadiummolybdophosphoric acid, used because of their good redox and acid/base properties, are, for example, catalyst precursors for the oxidative dehydrogenation reaction of isobutyric acid to methacrylic acid [1-3]. Unfortunately, however, the title compound in particular with x = 0, is thermally unstable, which makes it especially difficult to determine the catalytically active center. Many efforts have been made to investigate the thermally unstable state, for example, by XRD [2,4], TG-DTA coupled with IMR-MS and DSC [2,5], IR [4, 6-8], EPR [9,10] and Raman [11-13]. To improve the stability and catalytic activity of such compounds, cations were introduced in the secondary structure [14, 15]. Recently, the caesium containing compound with x = 2 proved to be the best catalyst among the different title compounds, for instance for the partial oxidation of ethene and propene by molecular oxygen [14-16]. An important role in the structural dynamics of this type of compound is played by the reducibility of the cationic centres, which was investigated by EPR spectroscopy [10]. Changes in the redox state of heteropoly compounds can also be investigated by the UV/Vis/near-IR spectroscopy. In the case of gas/solid reactions this method is restricted to the reflectance mode because the absorption in the catalyst samples, which must have a certain necessary thickness, is too high. During changes in the redox state the spectroscopic characteristics, such as the number of the absorption bands, peak positions and band gap energies, also change. Besides the oxygen ligand to metal charge transfer band (LMCT) there are absorption bands which can develop or disappear due to the optical d-d transitions in $V^{4+}$ and $Mo^{5+}$ and intervalence $V^{4+}$ - $Mo^{6+}$ and/or $Mo^{5+}$ - $Mo^{6+}$ optical transitions. Up to now, this spectroscopic method has been applied to the investigation of heteropoly compounds by some work groups, but all spectra were recorded ex situ [17-21]. The heteropoly compounds alter the spectroscopic behaviour due to the loss of water [22, 23]. In certain compounds of this type, even a small water loss leads to noticeable changes in the absorption band intensity. The resulting strong alterations of light absorption can only be observed with improved spectroscopic equipment [24].

We report here on a systematic in situ study of the influence of both an inert gas (He) and other gas atmospheres ($O_2$, propene, $O_2$/propene) on the spectroscopic feature at room temperature and higher temperatures, respectively. The goal of the paper is also to find out a correlation be-

tween the spectroscopic characteristics and catalytic data for the oxidation of propene on the title compounds.

In [25] a model was worked out for the calculation of the charge transfer and d-d -bands arising from the homonuclear $Mo^{5+}$-$Mo^{6+}$ and heteronuclear $V^{4+}$-$Mo^{6+}$ pairs in intact and ill-defined fragments of the Keggin structure contributing to the absorption spectra under different experimental conditions. Electron transfer processes $V^{4+}$-O- $Mo^{6+}\rightarrow$ $V^{5+}$-O- $Mo^{5+}$ , $Mo^{5+}$-O- $Mo^{6+}\rightarrow$ $Mo^{6+}$-O- $Mo^{5+}$ involving two metal centers were taken into consideration. The vibronic coupling constants and crystal field splittings determining the positions and the shapes of the charge transfer and d-d bands were calculated in the exchange charge model [26] of the crystal field. In the present paper on the basis of the established in [25] regularities a qualitative explanation of the temperature behaviour of the visible (Vis) and NIR parts of the absorption spectra of $H_{4-x}Cs_x$ $PVMo_{11}O_{40}$ (x=0,2) will be given. Along with this, the band gap energies that change with different gas atmospheres will be determined as a function of temperature.

## 2. Experimental

A Perkin-Elmer Lambda 9 spectrometer with an enlarged integrating sphere and a flow-through microreactor was used for in situ UV/Vis/near-IR diffuse reflectance spectroscopy on different dilute catalyst samples up to 663 K. In the home-made flow-through microreactor, temperature gradients in the catalyst bed of up to 30 K were registered at the highest temperatures. Approximately 110 mg of the catalyst were mixed with $SiO_2$ (Heraeus, 0.1- 0.4 mm) (7-10 wt.-%) and placed in a home-made microreactor operating under continuous gas flow. All spectroscopic measurements were carried sequentially out with a scan speed of 240 nm/min, a slit width of 5.0 nm and a response time of 0.5 s, as well as with a spectralon as a reference.

The free heteropoly acid ($H_4PVMo_{11}O_{40}$), denoted as HPA, was prepared by hydrothermal synthesis from stoichiometric mixture of metal oxides ($MoO_3$, $V_2O_5$) and phosphoric acid in water. $Cs_2CO_3$ and the solution of heteropoly acid were used for the preparation of the $Cs_2$ salt ($Cs_2H_2PVMo_{11}O_{40}$), denoted as $Cs_2A$.

The gases used were helium (purity > 99.999 vol.-%), helium saturated with water at room temperature (RT) and oxygen (purity > 99.998 vol.-%). In addition, the feed mixture was 10 vol-% propene (purity ≥ 99.8 vol.-%) in helium or 10 vol-% propene plus 10 vol-% oxygen in helium with a total gas flow of 71 or 74 ml/min, respectively. Oxygen, propene and the reaction products were analyzed on-line with two gas chromatographs (Perkin Elmer), equipped with heated automatic gas sampling valves, an FFAP column (Macherey-Nagel) and a packed Carboxen-1000 column using an FID and an TCD.

Three different methods of gas atmosphere treatment were applied for spectra recording. First, He treatment was carried out for about 12 hours at RT. Second, propene/He treatment was carried out for about 2 hours at RT, and then the temperature was increased at a rate of 1 K/min to 323 K, and the spectra were recorded over a period of ca. 5 hours. Third, an isochronic-isothermic temperature-time program was chosen for all gas atmospheres as follows: gas atmosphere treatment for ca. 2 hours at RT, whereby $RT_1$ denotes the initial spectrum and $RT_2$ the spectrum after 2 hours on gas flow. Then the temperature was increased from $RT_2$ to 326 K with a heating rate of 1 K/min and of this temperature to 663 K in steps of ~ 50 K with the same heating rate, with a holding time of 2 hours for each gas at each temperature.

For all operations described in sections 3 and 4, the last spectrum was always taken before the temperature was increased. The holding time of 2 hours was sufficient because no spectroscopic changes were observed after this time. The apparent absorption was evaluated from the diffuse reflectance data using the formula $1\text{-}R_{mixture}/R_{SiO2}$, whereby at each desired temperature the measured reflectance data of the mixture were divided by the pure $SiO_2$ diluent. For some spectra it was necessary to eliminate the jumps close to the lamp (ca. 320 nm) and the detector change (ca. 860 nm). In addition, the reflectance data in short wavelength ranges near these particular points were smoothed.

## 3. Determination of spectroscopic characteristics

From Figure 1 it is seen that above 326 K, the intensity of the spectra increases significantly both in the Vis and near-IR range. The investigation of Raman spectra [13] shows that the formation of ill-defined clusters takes place at higher temperatures. Therefore the transformations of the spectra in the range 326 < T < 663 K are attributed to these clusters. Correspondingly, the spectral intensities were determined by integration in the range of A < λ < B, where A is the lowest point of the band edge and B is 2000 nm.

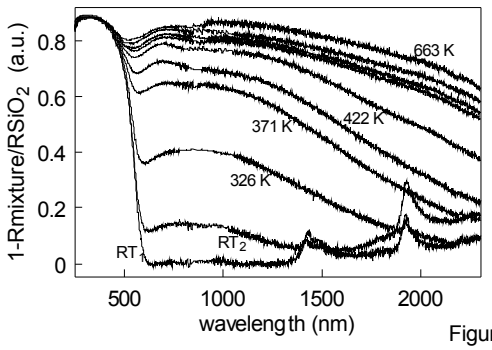


Figure 1

Figure 1: Spectroscopic screening for $He/H_2Cs_2PVMo_{11}O_{40}$ from RT to 663 K. $RT_1$ : RT, He flux : 6 min; $RT_2$ : RT, He flux 105 min

The upper limit of this interval was determined in correspondence with the results obtained in reference [25] which showed that the maximum of the lower energy intervalence charge transfer band arising from ill-defined dimeric clusters is about 2000 nm. For fixed temperatures the relative spectrum intensity was determined as $n = I_i/I_0$ where $I_i$ and

$I_0$ are the intensities of spectra at temperatures T and T = 663 K. The peak positions of the absorption bands were evaluated after a linear background subtraction. The spectra of heteropoly compounds in the range of light-induced LMCT are usually interpreted as interband optical transitions or transitions between discrete molecular orbitals. However, we employ the band model bearing in mind two factors. Firstly, the disintegration of heteropoly compounds examined is accompanied by water removal (crystal or constitutional water). Independent of the stage of disintegration of the Keggin units, the mean geometric distance between them decreases. This facilitates polymerisation and thus interunit electron transfer. Secondly, the final product of disintegration is the semiconductor $MoO_3$. The filled valence band and the conduction band are formed by the oxygen 2p and metal d orbitals [27], respectively. At the beginning of the experiment ($RT_1$, short time on gas flux), when the intervalent charge transfer and d-d bands are not yet developed, the absorption band edge is determined as a point at which the slope of the apparent absorption coefficient for the LMCT band is at its maximum. At higher temperatures in the range of 400 - 600 nm the overlap of the LMCT band, d-d and IVCT bands becomes appreciable, and this procedure does not lead to reasonable results. Therefore, for temperatures above $RT_1$ we evaluate the shift of the absorption band edge relative to its position under the initial experimental conditions. Assuming that for direct interband optical transitions the apparent absorption coefficient is a function f of $\hbar\omega$-Eg (where $\hbar\omega$ is the photon energy, and Eg is the optical band gap energy) at different temperatures we estimate the values $\hbar\omega$ corresponding to a fixed value of f equal to $f_0$ and taken in the vicinity of the maximum of the LMCT band, i.e., in the range within which the UV absorption is not affected by the d-d and IVCT transitions. The change $\hbar\Delta\omega$ in the photon energy determined in this way is equal to the shift $\Delta$Eg of the absorption band edge.

## 4. Results and Discussion

### 4.1. Peak intensity versus time on He stream at room temperature

The loss of crystal water can be observed from the change of the near-IR absorption bands at 1430 and 1930 nm. Such a water loss, recognizable in the decreasing peak intensity, is already observed at RT in dependence upon time on He stream, as can be seen in Figure 2. In addition, in the ultraviolet spectral range HPA and $Cs_2A$ exhibit pronounced LMCT bands at ca. 400 and 360 nm, respectively. The intensity and the shape of this band do not change during the action of the He stream. In the Vis/NIR range an asymmetrical broad band is observed, whose peak intensity increases with increasing time on He stream. The peak maximum of this band is located in the range of 740-780 nm and a shoulder can be distinguished in the range of 900-1000 nm. A semiempirical model that considers a dimeric cluster $V^{4+}$-$Mo^{6+}$ was employed for the simulation of the spectra [28]. At 300 K under He the spectra of HPA in the Vis/NIR range were shown to be determined by the optical d-d transitions in $V^{4+}$ and $Mo^{5+}$ ions with intact oxygen surroundings ($MO_6$) and the intervalence transition $V^{4+}$-$Mo^{6+}$. The maximum observed in the range 740-780 nm (Fig. 2) was assigned to the intense $b_2$-e (d-d) transitions in $V^{4+}$ and $Mo^{5+}$. The shoulder in the range 900-1000 nm was assigned to an IVCT peak of the heteronuclear pair V-Mo.

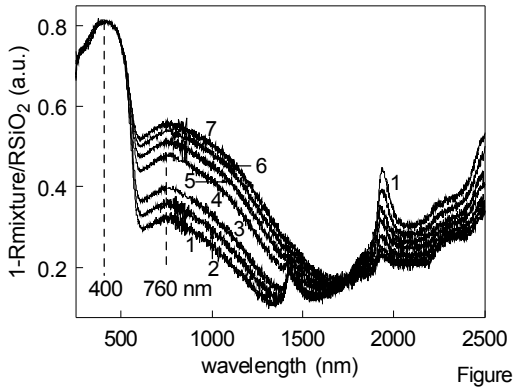


Figure 2

Figure 2 : Experimental UV/Vis/near-IR diffuse reflectance spectra of $H_4PV$- $Mo_{11}O_{40}$ in dependence upon time on He stream at room temperature.
time on stream (hours) : 1.4 (spectr. 1); 1.9 (spectr. 2); 2.4 (spectr. 3); 9.9 (spectr. 6); 12.3 (spectr. 7).

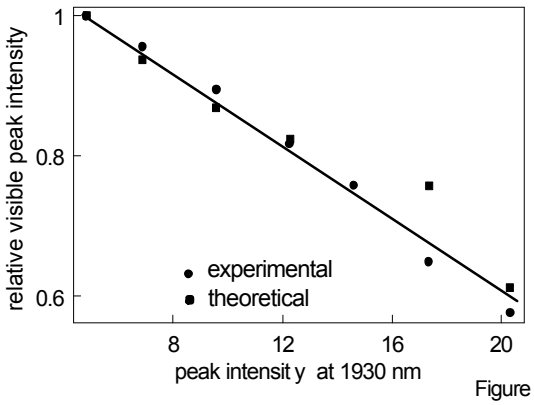


Figure 3

Figure 3 : Relative visible peak intensity of $He/H_4PVMo_{11}O_{40}$ at room temperature calculated from experimental and theoretical spectra vs. peak intensity at 1930 nm.

Appreciable spectroscopic changes between 600 and 1300 nm were attributed to the increase in the parameter characterising electron transfer between the $V^{4+}$ and $Mo^{6+}$ ions (electron transfer parameter) due to water loss. By varying of this parameter a good fit of the calculated spectra on the experimental ones could be obtained [28]. Besides the electron transfer parameter all other characteristic system parameters were determined from experimental data. The theoretical calculations [28] make it possible to separate the contributions of the d-d transitions and the charge transfer band from the total spectrum intensity. At RT the relative contribution of the d-d-transitions decreases appreciably

with time on He stream, while the intensity of the charge transfer band grows with the increase in the transfer parameter. For example, for the spectrum recorded at RT after 12.2 hours on He stream these contributions are 34 (d-d) and 66 % ( charge transfer). In addition, it was determined that the peak intensity of the near-IR $H_2O$ absorption bands correlates with the peak intensity in the range indicated above. Figure 3 shows this connection for HPA treated in He selecting the greater near-IR $H_2O$ peak intensity at 1930 nm.

### 4.2. Spectroscopic screening in dependence upon the gas atmo-sphere and temperature

For $Cs_2A$ treated in He from RT to 663 K the apparent absorption increases strongly with the temperature (Fig. 1). Such an increase in UV/Vis was already shown and discussed in [22]. Simultaneously, the near-IR absorption bands of the crystal water disappear completely, with the consequence that a Vis broad absorption band, and at higher temperatures additionally a near-IR absorption band can be clearly detected. A similar feature is observed for HPA in the pre-sence of He. In contrast, the spectroscopic feature for HPA and $Cs_2A$ is different in the presence of propene or the mixture of $O_2$/propene instead of He. After a time on stream of 2 hours the apparent absorption already increases enormously at RT in the presence of propene. No water band could be detected any longer in the presence of propene for $Cs_2A$ after this time at RT and for HPA after 2 hours at 326 K (not shown). The reason for the very strong increase in the apparent absorption in the presence of propene is that propene apparently draws the crystal water from the catalyst, and when that has disappeared the constitutional water as well. The Vis peak position suffers a blue shift from 740 nm to 700 nm after a time on stream of ca. 90 min with a slight temperature increase (to 319 K) (not shown), accompanied by the formation of iso-propanol detected by GC**.** In the presence of $O_2$ the increase of the apparent absorption is not as strong as in the case of He and the removal of water molecules proceeds more slowly with increasing time on stream and temperature. In addition, for HPA treated in $O_2$ no successive increase of the apparent absorption is observed with increasing temperature, so that, for instance, the apparent absorption in a certain temperature range can be greater than at higher temperatures. He saturated with water appears to have a stabilizing action on these compounds. The water bands disappear only at 473 K (not shown).

### 4.3. Influence of gas atmospheres on the visible and near-IR peak intensity between RT and 663 K

With the exception of $He/H_2O$, the Vis and near-IR peak intensity increase strongly in the presence of the gas atmospheres applied up to 373 K, as can be seen in Figures 4 and 5. The initially dramatic change in the Vis and near-IR peak intensity points to the crystal water loss which already begins at RT (see section 4.1) and continues up to 400 - 420 K. A lower change in peak intensity is observed in the range 520 -540 K (see Figs. 4 and 5), wherein the constitutional water loss begins **[**14,15**]**.

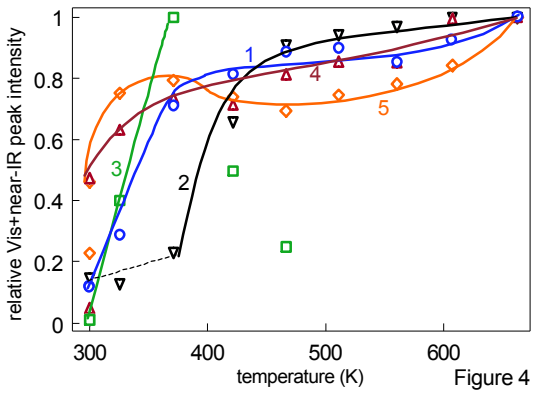


Figure 4 : Influence of gas atmospheres and temperature on the relative visible and near-IR peak intensity of $H_4PVMo_{11}O_{40}$.
1 : He; 2 : $He/H_2O$; 3 : $O_2$; 4 : propene; 5 : $O_2$/propene

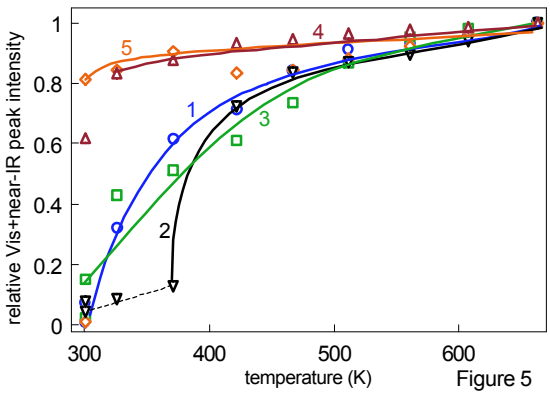


Figure 5 : Influence of gas atmospheres and temperature on the relative visible and near-IR peak intensity of $H_2Cs_2PVMo_{11}O_{40}$.
1 : He; 2 : $He/H_2O$; 3 : $O_2$; 4 : propene; 5 : $O_2$/propene

As already mentioned in section 4.2., the strongest increase can be recognized for both catalysts in the presence of propene and the mixture of $O_2$/propene up to 373 K. In contrast, the peak intensity rapidly decreases for HPA in the presence of $O_2$ above 373 K, and above 473 K no peak intensity was observed. For $Cs_2A$ the peak intensity increases similarly to the increase in the presence of He. However, the peak intensity is lower than that of He in the range 350-500 K. Another peak intensity vs. temperature curve is observed in the presence of $He/H_2O$. A clear increase of this intensity can only be detected above 373 K.
For HPA the decrease in the peak intensity of the Vis and near-IR absorption band above 373 K (Fig. 4) in the presence of $O_2$ may be attributed to an oxidation of $Mo^{5+}$ and $V^{4+}$ centers by this gas phase. For HPA the $O_2$ produces such a strong oxidation that no more absorption bands could be identified. In contrast, the $Cs^+$ ions play a stabiliz-

ing role in the $Cs_2A$ salt and hinder significant oxidation. Above 513 K, for HPA the Vis and near-IR peak intensity increase under reaction conditions ($O_2$/propene).

### 4.4. Influence of gas atmospheres on the visible peak position bet-ween RT and 663 K

Figure 6 shows that the peak position of the Vis absorption band is blue shifted for HPA in the presence of He, the mixture of $O_2$/propene, or propene (strong shift) with increasing temperature. For $Cs_2A$ in the presence of these gas atmospheres, the spectroscopic feature is the same up to 373 K (propene), 423 K (He) and ca. 473 K ($O_2$/propene), as can be seen in Figure 7. Above these temperatures the Vis peak positions are nearly constant (He, propene) or increase slightly ($O_2$/propene). In contrast, a Vis peak position for HPA treated in $O_2$ can only be observed up to 373 K, and for $Cs_2A$ treated in the same gas an increase is detected after a decrease up to 373 K. In the case of $O_2/Cs_2A$ two data sets show the same spectroscopic trend (see Fig.7). $He/H_2O$ appears to have a stabilizing effect up to ca. 373 K and 420 K for HPA and $Cs_2A$, respectively. If the crystal water is removed with increasing temperature one observes a blue shift of the Vis peak position that is stronger in the case of $Cs_2A$ than of HPA. However, such a shift is not detected for $Cs_2A$ with the exception of $He/H_2O$ in the temperature range in which the constitutional water is removed (see Figs. 6 and 7).

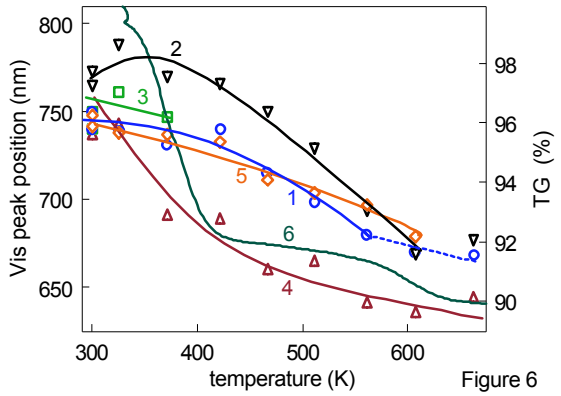


Figure 6

Figure 6 : Influence of gas atmospheres and temperature on the visible peak position and thermogravimetric behaviour (TG) of $H_4PVMo_{11}O_{40}$.
1 : He; 2 : $He/H_2O$; 3 : $O_2$; 4 : propene; 5 : $O_2$/propene
6 : TG curve recorded under $N_2/O_2$ atmosphere with 10 K/min [16]

The results obtained can be explained on the basis of calculations carried out in [25]. For a clearer understanding of the interpretation presented below we first give a short description of the background of the model employed [25]. Qualitative considerations [29], semiempirical [28, 30] and microscopic estimations [25] testify that the single-electron transfer between corner-sharing me-tal sites in the reduced Keggin unit is the leading one, while the corresponding transfer parameter p is small in comparison with the characteristic vibronic coupling parameters. This allows us to consider the tunnel interaction as a perturbation and to identify the stationary states of the system with those in which the excess electrons are localized.

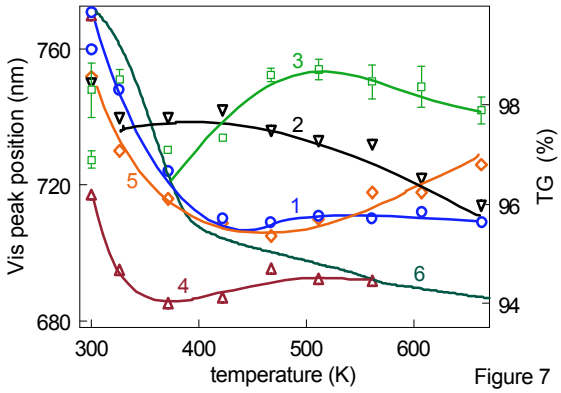


Figure 7

Figure 7 : Influence of gas atmospheres and temperature on the visible peak position and thermogravimetric behaviour (TG) of $H_2Cs_2PVMo_{11}$- $O_{40}$.
1 : He; 2 : $He/H_2O$; 3 : $O_2$ , two data sets are shown; 4 : propene; 5 : $O_2$/propene; 6 : TG curve recorded under $N_2/O_2$ atmosphere with 10 K/min [16]

On the other hand, the most intense IVCT bands of reduced heteropoly anions arise from transitions in which under action of light the only electron jumps from its original site to a neighbouring one. Hence, it follows that the problem of calculation of the IVCT band positions of the whole Keggin unit (intact or defective) may be reduced to that of light-induced electron transfer between two adjacent corner-sharing metal ions ($Mo^{5+}$, $Mo^{6+}$ or $V^{4+}$, $Mo^{6+}$). The full spectrum (i.e. the observed spectrum) of the Keggin unit can be obtained by summation over spectra originating from all possible single-electron transfers between neighbouring corner-sharing sites and d-d transitions in $Mo^{5+}$ and $V^{4+}$ ions, taking into account in each case the thermal population of the initial electron-vibrational state participating in the optical transition. The considerations given above led us to a study of optical electron transfer and d-d bands of binuclear clusters consisting of metal ions joined through an apex and containing a single electron over the filled shells of these ions (clusters $Mo^{5+}$-$Mo^{6+}$ or $V^{4+}$-$Mo^{6+}$). The calculation of the shapes and the positions of these bands was carried out in a realistic model of the crystal field taking into account both the electrostatic field of point charges of lattice ions and the exchange charge field [26] allowing for the covalency effects in the binding of the metal ions to the oxygens in the nearest coordination sphere.

Depending upon time on gas flux and temperature the nearest oxygen surrounding of a metal ion (M) in the Keggin unit may be unimpaired ($MO_6$) or ill-defined. Therefore, further the structure of reduced binuclear mixed-valence species responsible for the spectra transformations on different stages of the experiment will be denoted as $((O_t)_{1-s1}(O_p)_{1-y1}(O_b)_{3-x1}H_{a\ z1})d^1$-$O_b$-$d^0((O_t)_{1-s2}(O_p)_{1-y2}\ (O_b)_{3-x2}H_{b\ z2})$, where $O_b$, $O_t$ are the bridging and terminal oxy

Table 1: Calculated positions of the charge-transfer (CT) and d-d bands arising from different types of species in the Vis range
* this band is on the border of the Vis and near-IR range in temperature interval of crystal water loss

| species | band | temperature (K) | position (nm) |
|---|---|---|---|
| $(O_tO_p(O_{b)3}H_{b1})V^{4+}$-$O_b$-$Mo^{6+}(O_tO_p(O_b)_3)$ | CT | 330 | 830* |
| $(O_tO_p(O_{b)3})V^{4+}$-$O_b$-$Mo^{6+}(O_t(O_b)_3)$ | CT | 500 | 755 |
| $(O_t(O_{b)2})Mo^{5+}$-$O_b$- $V^{5+}(O_tO_p(O_b)_3)$ | CT | 500 | 750 |
| $(O_t(O_{b)2})Mo^{5+}$-$O_b$- $Mo^{6+}(O_tO_p(O_b)_3)$ | CT | 500 | 722 |
| $(O_tO_p(O_{b)2})Mo^{5+}$-$O_b$- $Mo^{6+}(O_tO_p(O_b)_2)$ | CT | 500 | 664 |
| $(O_t(O_{b)2})V^{4+}$-$O_b$-$Mo^{6+}(O_tO_p(O_b)_3)$ | CT | 500 | 600 |
| $(O_tO_p(O_{b)2})Mo^{5+}$-$O_b$- $V^{5+}(O_tO_p(O_b)_3)$ | CT | 500 | 552 |
| $(O_tO_p(O_{b)2})V^{4+}$-$O_b$-$Mo^{6+}(O_tO_p(O_b)_2)$ | CT | 500 | 543 |
| $(O_tO_p(O_{b)2})Mo^{5+}$-$O_b$- $Mo^{6+}(O_tO_p(O_b)_3)$ | CT | 500 | 537 |
| $(O_tO_p(O_{b)2})V^{4+}$-$O_b$-$Mo^{6+}(O_tO_p(O_b)_3)$ | CT | 500 | 457 |
| $(O_tO_p(O_{b)4})V^{4+}$ | d-d | | 769, 625 |
| $(O_tO_p(O_b)_4H_{b1})V^{4+}$ | d-d | | 743, 720, 519 |
| $(O_tO_p(O_{b)4})Mo^{5+}$ | d-d | | 712, 444 |
| $(O_tO_p(O_{b)4}H_{b1})Mo^{5+}$ | d-d | | 701, 505, 498 |

Table 2: Calculated positions of the charge-transfer bands in the near-IR range

| species | temperature (K) | band position (nm) |
|---|---|---|
| $(O_tO_p(O_{b)3}H_{b1})V^{4+}$-$O_b$-$Mo^{6+}(O_tO_p(O_b)_3H_{b1})$ | 340 | 922 |
| $(O_tO_p(O_{b)3})V^{4+}$-$O_b$-$Mo^{6+}(O_tO_p(O_b)_3)$ | 340 | 1012 |
| $(O_tO_p(O_{b)3}H_{b1})Mo^{5+}$-$O_b$-$Mo^{6+}(O_tO_p(O_b)_3)$ | 340 | 1011 |
| $(O_tO_p(O_{b)3}H_{b1})Mo^{5+}$-$O_b$-$V^{5+}(O_tO_p(O_b)_3)$ | 340 | 1068 |
| $(O_tO_p(O_{b)3}H_{b1})Mo^{5+}$-$Mo^{6+}(O_tO_p(O_b)_3H_{b1})$ | 340 | 1142 |
| $(O_tO_p(O_{b)3})Mo^{5+}$-$Mo^{6+}(O_tO_p(O_b)_3)$ | 340 | 1224 |
| $(O_tO_p(O_{b)3})V^{4+}$-$O_b$-$Mo^{6+}(O_p(O_b)_3)$ | 560 | 1091 |
| $(O_tO_p(O_{b)3})Mo^{5+}$-$O_b$-$V^{5+}(O_t(O_b)_3)$ | 560 | 1000 |
| $(O_p(O_{b)3})V^{4+}$-$O_b$-$Mo^{6+}(O_p(O_b)_3)$ | 560 | 980 |
| $(O_tO_p(O_{b)3})Mo^{5+}$-$O_b$-$Mo^{6+}(O_t(O_b)_3)$ | 560 | 873 |

gens, $O_p$ stands for the oxygen in a phosphorus tetrahedral environment, $d^1$ designates the 3d or 4d-electron, $s_i$, $x_i$ and $y_i$ are the numbers of oxygen ions extracted in the process of constitutional water or oxygen evolution, $z_i$ is the number of protons localized on the moiety, $a, b$ = b or t for protons residing on the oxygens $O_b$ and $O_t$, respectively. The composition of very likely species was chosen on the basis of the thermal gravimetric, differential thermal and IMR-MS analysis [2,23], geometric structure of $MoO_3$ and quantum-mechanical calculations of proton affinities [31]. The symmetry of the unimpaired units $MO_6$ comprising the cluster was assumed to be $C_{4v}$, the symmetry of the ill-defined moieties $M((O_t)_{1-si}(O_p)_{1-yi}(O_b)_{4-xi}H_{a\ zi})$ was taken in according with the scheme of reduction of the $C_{4v}$ group on the subgroups. The calculated maxima of charge transfer bands arising from intact and some ill- defined binuclear species are listed in Tables 1 and 2.

Quantum-mechanical calculations [25] show that reduced binuclear species with protons localized on the bridging oxygens (Tables 1, 2) or with vacancies of the bridging oxygens (Table 1) give blue shifted charge transfer bands relative to those arising from intact ones, a proton on the terminal oxygen leads to a red shift. The Vis part of the spectra in heteropolyacids and Cs-salts is revealed to be formed by d-d and IVCT transitions $V^{4+}$-O-$Mo^{6+}\rightarrow V^{5+}$-O-$Mo^{5+}$ , $Mo^{5+}$-O- $Mo^{6+}\rightarrow Mo^{6+}$-O-$Mo^{5+}$ (Table 1). Depending on temperature the IVCT transitions arise from species $(O_tO_p(O_{b)3}H_{b1})V^{4+}$-$O_b$-$Mo^{6+}(O_tO_p$ $(O_b)_3)$ with a proton localized on the bridging oxygen or reduced species of the type of $VMoO_{10}$, $VMoO_9$, $Mo_2O_{10}$, $Mo_2O_9$ with one or two oxygen vacancies [25] (Table 1).

At RT after a certain time on gas flux (for example, He (Fig. 2)) in HPA the loss of crystal water begins. At this initial stage there is no reduction, the HPA is partly in the hydrated phase, the protons are not localized and reside on the bridging water moieties $H_5O_2^+$. However, the quantitative determination of the $V^{4+}$ content by EPR [10] shows that even on this stage vanadium is present as $V^{4+}$, its amount is about 0.5-2 mol %. At the same time a small amount of $Mo^{5+}$ is also detected. Therefore initially, the

Vis part of the spectra originates mainly from the d-d transitions in the contained $V^{4+}$ and $Mo^{5+}$ ions [28]. The total spectrum intensity increases due to the increase of the intensity of the charge transfer band arising from the $V^{4+}$-$Mo^{6+}$ intervalent transition in intact species $VMoO_{11}$ [28] that contributes to the first near-IR band (see Table 2 and section 4.5). At temperatures 326-420 K the removal of crystal water (see thermogravimetric Tg curves [16] in Fig. 6 and 7) is accompanied by the localization of acidic protons the most energetically favourable sites of which have been shown to be the bridging oxygens [31,32]. All reduced species with protons residing on the bridging oxygens listed in Tables 1 and 2 give rise to new d-d transitions blue shifted in comparison with those arising from intact $VMoO_{11}$ clusters (Table 1). Besides this, at temperatures 326-420 K on the border of the Vis and near-IR range a new charge transfer band originating from the $(O_tO_p(O_b)_3H_{b1})V^{4+}$-$O_b$-$Mo^{6+}(O_tO_p\ (O_b)_3)$ species appears (Table 1). On the other hand, with temperature rise in the range of crystal water loss the concentration of reduced protonated species increases as fast as the protons localize on the oxygens of the reduced intact species. Both mentioned factors lead to the observed gradual blue shift of the Vis peak position in HPA and $Cs_2A$ (Figs. 6 and 7). At the same time the spectra intensity increases due to increase of the transfer parameter with water loss. However, in spite of the smaller number of localized protons for $Cs_2A$ in the range of crystal water loss the blue shift of the Vis band is of the same order for HPA and $Cs_2A$. This can be explained by the stronger crystal field and electron-vibrational coupling in $Cs_2A$.

As the temperature continues to rise, constitutional water evolves (see thermogravimetric Tg curves [16] in Figs. 6 and 7). This water is formed by the extraction of an oxygen by two protons and leads to the formation of defective clusters in which bridging oxygens are removed. However, the constitutional water evolution itself is not accompanied by the appearance of new reduced clusters. Therefore, at this stage the transformations of the spectra may occur due to the reduced species of the type of $VMoO_{10}$, $VMoO_9$, $Mo_2O_{10}$, $Mo_2O_9$ enumerated in Table 1 and formed from reduced protonated species. Meanwhile, the evolution of molecular oxygen may lead to the formation of the same clusters $VMoO_{10}$, $VMoO_9$, $Mo_2O_{10}$, $Mo_2O_9$ from intact non-reduced $VMo_{11}$, $Mo_2O_{11}$ ones. The indicated ill-defined species promote a further blue shift of the Vis band. Their concentration increases with temperature rise, and the total intensity of the Vis part of the spectra grows. After crystal water removal for $Cs_2A$ the position of the Vis band remains nearly unchanged insofar as, due to the structure of this compound, the number of species with oxygen vacancies formed in the course of constitutional water release is approximately two times smaller than in HPA. The propene atmosphere leads to the same effects in the Vis part of HPA and $Cs_2A$ spectra. However, propene is more efficient in the extraction of water than He, which is due to the additional reaction leading to the product isopropanol. Therefore, for propene/HPA the Vis band shift is larger, and in $Cs_2A$ the Vis peak position stabilizes at lower temperatures.

Under action of $O_2$ the band in the Vis part of the HPA spectrum disappears after the crystal water loss. At the same time under $O_2$ flux in $Cs_2A$ salt the Vis peak can be observed from RT to 663 K, and this is due to the presence of $Cs^+$ ions which prevent oxidation.

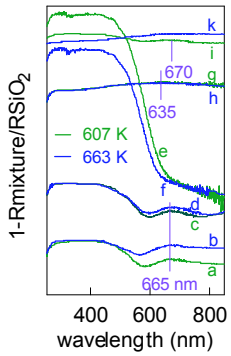


Figure 8

Figure 8 : Influence of gas atmospheres on the in situ UV/Vis spectra of $H_4PV$-$Mo_{11}O_{40}$ at 607 and 663 K.
a, b : He; c, d : He/$H_2O$ ; e, f : $O_2$; g, h : propene; i, k : $O_2$/propene
For a better visualization the spectra were vertically shifted.

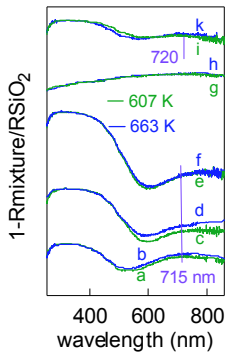


Figure 9

Figure 9 : Influence of gas atmospheres on the in situ UV/Vis spectra of $H_2Cs_2P$-$VMo_{11}O_{40}$ at 607 and 663 K.
a, b : He; c, d : He/$H_2O$; e, f : $O_2$ –one of the two $O_2/H_2Cs_2PVMo_{11}O_{40}$ data sets was used; g, h : propene; i, k : $O_2$/propene
For a better visualization the spectra were vertically shifted.

The spectroscopic changes in the UV/Vis range at the highest temperature (607 K, 663 K) are shown in Figures 8 and 9. HPA treated in He develops a clear absorption band at 665 nm (directly observed in the spectra, deconvoluted on two bands at 660 and 740 nm, see section 3). For $Cs_2A$ treated in He as well a broader absorption band at 715 nm (directly observed in the spectra deconvoluted on two bands at 680 nm and 770 nm, see section 3) is detected (not shown). At 663 K the Vis peak position for $Cs_2A$ treated in He (see Fig. 7 ) is close to that of HPA, permitting the conclusion that $MoO_3$ and $Cs_3A$ salt are formed from $Cs_2A$ in good agreement with an in situ XRD result [33] and with a Raman shift of the main Keggin band from 988 $cm^{-1}$ for $Cs_2A$ to 992 $cm^{-1}$ for $Cs_3A$ [13]. This spectroscopic feature

indicates an expel of vanadyl species based on the calculated peak maximum at 660/740 nm for HPA and 680/770 nm for $Cs_2A$. These conclusions can also be drawn on the basis of observed absorption bands of $VOSO_4 \cdot 5H_2O$ at 625 and 766 nm [34]. However, corresponding Raman bands indicating vanadyl species could not be observed for these catalysts treated in He [13].

The absorption band at 665 nm which is observed in the presence of He disappears in the presence of $O_2$ for HPA (see Fig. 8). It also suffers a red shift and is weaker for $Cs_2A$ treated in $O_2$. As to the Vis peak position in $Cs_2A$ it can be recognized that this position regains its $RT_2$ value at higher temperatures. Hence, the presence of molecular $O_2$ could stabilize the $Cs_2A$ structure. In HPA $He/H_2O$ effects an even stronger Vis absorption band at ca. 665 nm in comparison to pure He. In this case the expel of vanadium species seems to be clearer still in contrast to the Raman observation (no corresponding bands). For $Cs_2A$ treated in $He/H_2O$ a weaker Vis band, which is red shifted, could indicate to a smaller number of expelled vanadyl species. HPA treated in propene shows a very broad weak absorption band with a observed peak maximum at ca. 635 nm and 2 deconvoluted spectra whose peak maxima are around 520 and 650 nm (not shown). In contrast, for $Cs_2A$ treated in propene as for HPA in the presence of $O_2$/propene at 665 K no peak positions could be certainly detected. An observed blue shifted peak position does not exist in the presence of the mixture of $O_2$/propene, either for HPA or $Cs_2A$. At ca. 605 K for HPA and $Cs_2A$, peaks can be recognized at ca. 670 nm and 720 nm, respectively. However, at the highest temperature of 665 K only a very broad weak absorption band is detected for $Cs_2A$. This weak absorption band has a nearly symmetrical shape with the peak maxima of ca. 720 nm ($Cs_2A$) and can be fitted exactly by one Gauss curve. The bands at 670 nm (HPA, 605 K) and 720 nm ($Cs_2A$ , 605 K, 665 K) point once again to vanadyl species. Raman spectra show bands at 1030 $cm^{-1}$ and 1008/1002 $cm^{-1}$ which were assigned to both vanadyl (HPA) and to molybdenyl species (HPA, $Cs_2A$) [13]. In addition the peak intensities of the Vis absorption band for HPA are obviously lower than that of $Cs_2A$ indicating the lower conversion of $O_2$ (see Figs. 8 and 9 and section 4.3.) [16]. One can conclude that $Cs_2A$ is structurally and electronically much more stable than HPA.

### 4.5. Influence of gas atmospheres on the near-IR peak position between RT and 663 K

The first near-IR peak position (that is the near-IR peak position with the lower wavelength in comparison with the second near-IR peak position) in the pre-sence of He, $He/H_2O$, propene or the mixture of $O_2$/propene shows a maximum for HPA between 473 K and 550 K, as can be seen in Figure 10. Using $O_2$ this peak position is only observed up to 473 K. However, in HPA above this temperature range a blue shift is detected in the presence of He, $He/H_2O$, propene and the mixture of $O_2$/propene. The HPA in the presence of $O_2$ shows a blue shift up to 423 K**.** Only $He/H_2O$ points to a stabilizing effect up to ca. 423 K for HPA.

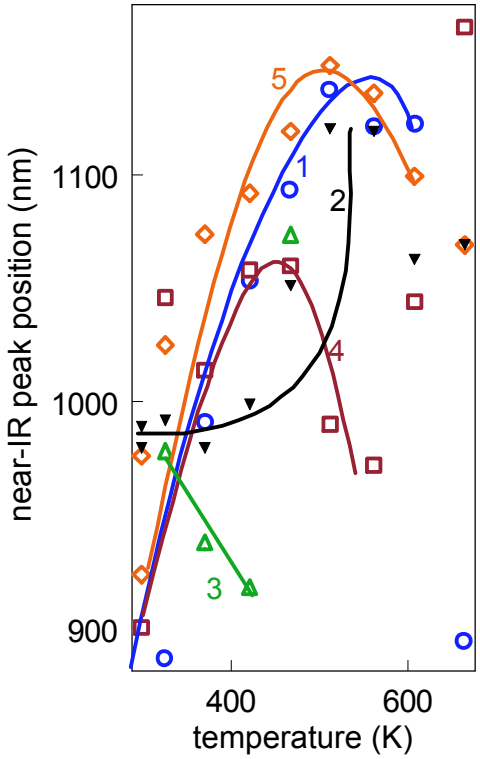


Figure 10

Figure 10 : Influence of gas atmospheres and temperature on the near-IR peak position of $H_4PVMo_{11}O_{40}$.
1 : He; 2 : $He/H_2O$; 3 : $O_2$ , two data sets are shown ;
4 : propene; 5 : $O_2$/propene.

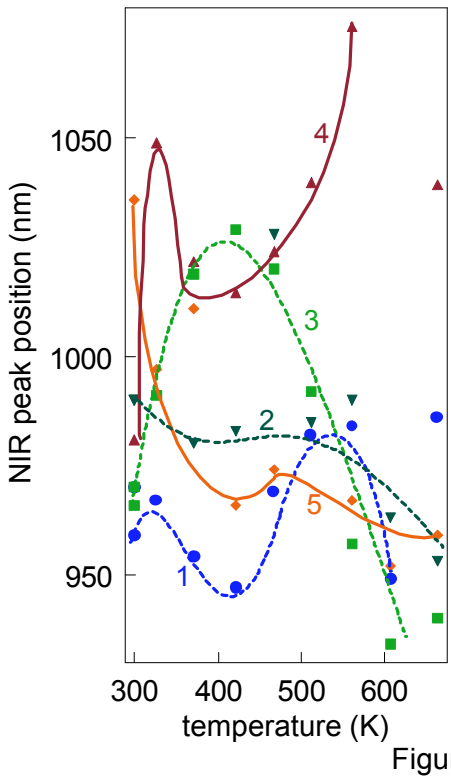


Figure 11

Figure 11 : Influence of gas atmospheres and temperature on the near-IR peakposition of $H_2Cs_2PVMo_{11}O_{40}$.
1 : He; 2 : $He/H_2O$; 3 : $O_2$; 4 : propene; 5 : $O_2$/propene

A decrease of the near-IR peak position is detected for $Cs_2A$ after 423 K in the presence of $He/H_2O$ and over the whole temperature range for the mixture of $O_2$/propene whereas under He, after a decrease the peak position again reaches a maximum between 470 K and 570 K, as can be seen in Figure 11. The propene near-IR peak position increases up to 520 K, and $O_2$ yields a broad maximum around 405 K. For $O_2/Cs_2A$ two data sets are presented in Fig. 11. The differences in the peak positions estimated from these data sets are insignificant up to 570 K. In this a way it is confirmed that for temperatures lower than 570 K the trend in behaviour of the near-IR position for $O_2/Cs_2A$ can be reproduced.

The second near-IR peak position has not been plotted and discussed here in so far as it is difficult to determine definitely the position of this band due to its strong overlap with the first near-IR band.

On the basis of quantum mechanical calculations [25] it can be concluded that independent of the gas atmosphere ($O_2$/propene, He or $He/H_2O$), the main trend in the temperature behaviour of the first near-IR band of the HPA consists in the following: At RT the first near-IR band originates from the heteronuclear intervalent transitions $V^{4+}$-$Mo^{6+}$. In the range of temperatures in which crystal water is removed (T~326-420 K) the main contribution to the near-IR band is provid-ed by the homonuclear $Mo^{5+}$-$Mo^{6+}$ and heteronuclear $V^{4+}$ - $Mo^{6+}$ intervalent transitions in reduced species $(O_tO_p(O_{b)3}H_{b1})V^{4+}$-$O_b$-$Mo^{6+}(O_tO_p$ $(O_b)_3H_{b1}$ ),
$(O_tO_p(O_{b)3}H_{b1})Mo^{5+}$-$O_b$-$Mo^{6+}(O_tO_p(O_b)_3)$,
$(O_tO_p(O_{b)3}H_{b1})Mo^{5+}$-$O_b$-$V^{5+}(O_tO_p$ $(O_b)_3)$,
$(O_tO_p(O_{b)3}H_{b1})Mo^{5+}$-$O_b$-$Mo^{6+}(O_tO_p$ $(O_b)_3$ $H_{b1})$ with acidic protons localized on the bridging oxygens (Table 2). In [25] it was shown that among these species the latter three are the most probable ones**.** The maxima of the charge transfer bands arising from the species $(O_tO_p(O_{b)3}H_{b1})Mo^{5+}$-$O_b$-$V^{5+}(O_tO_p$ $(O_b)_3)$, $(O_tO_p(O_{b)3}H_{b1})Mo^{5+}$-$O_b$-$Mo^{6+}(O_tO_p$ $(O_b)_3$ $H_{b1})$ are red shifted in comparison with those arising from $VMoO_{11}$ species. However, the maximum of the band originating from the species $(O_tO_p(O_{b)3}H_{b1})Mo^{5+}$-$O_b$-$Mo^{6+}(O_tO_p(O_b)_3)$ is close to that of $VMoO_{11}$ species. As a result a red shift of the near-IR band is observed in the range of crystal water loss. At the same time the increase of the transfer parameter with water loss promotes the increase of the band intensity. Then at higher temperatures before constitutional water release and oxygen evolution a further red shift of the maximum of the near-IR band takes place, and this is in agreement with the usual behaviour of charge transfer bands with rising temperature [28]. Further temperature increase leads to the evolution of constitutional water and molecular oxygen. The newly appeared reduced species, for instance of the type of $(O_tO_p(O_{b)3})V^{4+}$-$O_b$-$Mo^{6+}(O_p(O_b)_3)$, $(O_tO_p(O_{b)3})Mo^{5+}$ - $O_b$-$V^{5+}(O_t(O_b)_3)$, $(O_p(O_{b)3})V^{4+}$-$O_b$-$Mo^{6+}(O_p$-$(O_b)_3)$, $(O_tO_p(O_{b)3})Mo^{5+}$-$O_b$-$Mo^{6+}(O_t(O_b)_3$ ) (Table 2) cause a blue shift of the near-IR band. At a time with reduction the intensity of the near-IR band increases.

Under He the $Cs_2A$ salt demonstrates a different behaviour from the HPA behaviour of the near-IR peak position. The maxima of the bands arising from protonated clusters are higher in energy than those in acids. This may result in a slight blue shift of the near-IR peak position in the range of 326-420 K. Then, for temperatures 420-560 K, the red shift of the band may be explained by the usual temperature dependence of the charge transfer bands. The stabilization of the peak position at higher temperatures points to the fact that in Cs salts the number of ill-defined species formed under constitutional water removal is much smaller than in acids.

### 4.6. Influence of gas atmospheres on the band gap energy bet-ween RT and 663 K

The band gap energy values for HPA and $Cs_2A$ under different gas atmospheres are presented in Figure 12 as a function of temperature. For HPA treated in He, the band gap energy decreases in the temperature range $RT_1$ – 607 K. For $Cs_2A$ under He flow a decrease of the band gap energy is observed up to 570 K, and after which it remains unchanged. HPA and $Cs_2A$ treated in $He/H_2O$ show quite a different behaviour. For HPA after an increase in the band gap energy up to 371 K, a steep decrease in this energy is detected. For the $Cs_2A$ salt under $He/H_2O$ flux only a decrease in the band gap energy takes place. Both catalysts show a largely similar gap feature in pure $O_2$ : in the range $RT_1$ - 470 K a decrease in the band gap energy is observed.

At higher temperatures an increase occurs for HPA, whereas, in contrast, the band gap energy remains approximately constant for $Cs_2A$. For HPA and $Cs_2A$ under the propene/$O_2$ atmosphere the band gap energy decreases with temperature increase up to 570 K for HPA and 600 K for $Cs_2A$. At higher temperatures it is impossible to indicate a straight trend in temperature dependence for $Cs_2A$. It should also be mentioned that for both catalyts the band gap energy undergoes the maximum change under action of propene/$O_2$ flux. In addition, for both catalysts the band gap energies were not determined for propene atmosphere because of the very high apparent absorption in the relevant wavelength range. For the temperature behaviour of the absorption band edge under He stream, the following qualitative explanations may be given: Due to the peculiarities of the d electrons the conduction band formed by their orbitals can be described by the approximation of strong coupling. In this approximation the width of the conduction band is proportional to the hopping integral. With loss of water the mean distance between neighbouring units diminishes, and the overlap of their wave functions increases. This in turn leads to an increase in both the hopping integral and the width of the conduction band. In consequence, the width of the forbidden band and the absorption band edge decrease. In the case of $He/H_2O$ flux, the following interpretation may be proposed for the thermal behaviour of the band gap energy in HPA. The increase of the optical band gap at the initial stage evidences the decrease of the

width of the conduction band due to the additional external hydration of the system. It is clear that at this stage, the water of the flux prevents crystal water loss. The action of the water flux turns out to be stronger than that of He and temperature. Further temperature increase in common with He stream suppresses the hydration of the system by flux ($H_2O$ from flux) and facilitates the release of water. Therefore, further a decrease in band gap energy is observed for HPA. Under He/$H_2O$ the $Cs_2A$ salt does not show an initial increase of the optical band gap because the water coordination to $Cs^+$ ions is obstructive. The results obtained also show that in a wide temperature range for both catalysts under $O_2$ flux the "drying" effect of temperature exceeds that of $O_2$ ,which consists in oxidation of the reduced ions. At higher temperatures the number of electrons in the d band decreases appreciably due to oxidation. This promotes an apparent increase in the band gap energy in HPA. The action of propene removing the water proves to be stronger than that of oxygen. That is why the band gap energy decreases under propene/$O_2$ atmosphere.

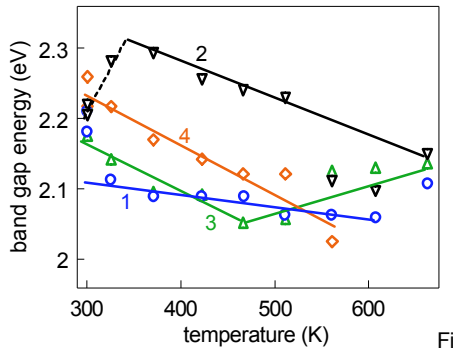


Figure 12a

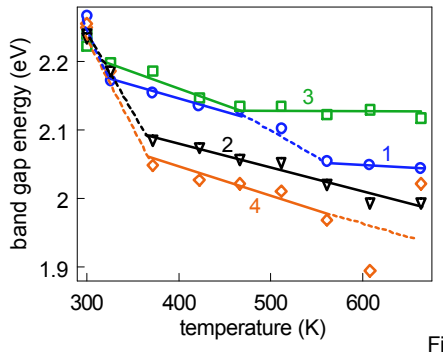


Figure 12b

Figure 12 : Influence of gas atmospheres and temperature on the band gap energy of $H_4PVMo_{11}O_{40}$ (a) and $H_2Cs_2PVMo_{11}O_{40}$ (b).
1 : He; 2 : He/$H_2O$; 3 : $O_2$; 4 : $O_2$/ propene.

### 4.7. In situ catalytic and spectroscopic experiments of $O_2$/pro-pene on HPA and $Cs_2A$

At 513 K on HPA a reaction and at 613 K on $Cs_2A$ a catalytic reaction occurs with a very low product concentration of acrolein and acetic acid in the reaction gas stream. At still higher temperatures, the conversion increases and in addition to these products propanal, acetone and CO are detected [16]. The conversion of propene on HPA at 513 K and 613 K is ca. 3% (no conversion change) and that of $O_2$ ca. 0.3% and 2%, respectively (Table 3) . On $Cs_2A$ at 613 K (first evidence of oxidation products) the conversion of propene is ca. 3% and that of $O_2$ ca. 12%, and the greatest selectivities were determined for acrolein and CO as may be seen in Table 4. It can be clearly recognized that for the propene oxidation on HPA the lattice oxygen is selective and the gas phase oxygen is unselective. In addition, it may be concluded from the catalytic data of the Table 3 that for HPA a catalytic reaction begins only above 573 K. The transition between the lattice and gas phase oxygen reaction cannot be recognized because a small reduction of the HPA catalyst continues above 573 K as well (Table 3). For $O_2$/propene on $Cs_2A$ one can determine the desired spectroscopic quantities (Vis peak position and band gap energy) only at 613 K (lowest reaction temperature). Above this temperature the low signal/noise ratio, large broadening and significant overlap of the bands prevent from the determination of the mentioned spec-troscopic characteristics. In contrast to the HPA investigations, gas phase oxygen appears only to be responsible for the $O_2$/propene reaction on $Cs_2A$ in the temperature range of 617 to 723 K because of the much higher $O_2$ conversion compared to that on HPA.

## 5. Conclusions

Spectroscopic characteristics represented as peak intensities, peak positions and band gap energies were determined for heteropoly compounds of the type of $H_{4-x}Cs_xPVMo_{11}O_{40}$ (with x=0,2) in the presence of different gas atmospheres in a wide range of temperatures. The obtained characteristics demonstrate an essential difference in the structural dynamics of HPA and $Cs_2A$ under action of different gas atmospheres. The nearly constant position of the Vis band in the range of constitutional water loss, the smaller values of the shifts of the near-IR band and sometimes opposite trends in the temperature behaviour of the band positions for $Cs_2A$ in comparison with HPA clearly evidence that the $Cs_2A$ compound remains stable up to higher temperatures than those for the acid. While comparing experimental data on $Cs_2A$ and HPA with the results of quantum-mechanical calculations [25] the types of reduced dimeric V-Mo, Mo-Mo clusters contributing to the formation of the Vis and NIR bands at different temperatures were identified. With the aid of the calculated positions of the d-d and charge transfer bands originating from intact and ill-defined reduced species the behaviour of the Vis and near-IR bands in the examined compounds with increasing temperature was qualitatively interpreted. In this connection, it should be mentioned that at high temperatures (520 K < T < 667 K ), especially for HPA treated in some gas atmospheres (He, He/$H_2O$) there is no clear trend, for example, in the temperature dependence of the Vis peak position. The following reasons can be enumerated. At high temperatures the latter cannot be singled out due to the

Table 3 : In situ catalytic and spectroscopic results in the propene oxidation on HPA after 1.5 h reaction time

| T (K) | conversion (%) | | selectivity (mol-%) | | | | | | spectroscopic quantities | |
|---|---|---|---|---|---|---|---|---|---|---|
| | propene | $O_2$ | acrolein | pro-panal | aceton | CO | acitic acid | by-product | visible peak position (nm) | band gap energy (eV) |
| 513 | 3 | 0,3 | 89 | -- | -- | -- | 9 | 2 | 706 | 2.05 |
| 573 | 3 | 0,3 | 40 | -- | -- | 51 | 8 | 1 | 692 | 2.0 |
| 613 | 3 | 2 | 34 | 30 | 6 | 25 | 4 | 1 | 679 | 1.96 |
| 665 | 12 | 6 | 24 | 13 | 6 | 29 | 26 | 2 | --- | --- |

Table 4 : In situ catalytic and spectroscopic results in the propene oxidation on $Cs_2A$ after 1.5 h reaction time

| T (K) | conversion (%) | | selectivity (mol-%) | | | | | | spectroscopic quantities | |
|---|---|---|---|---|---|---|---|---|---|---|
| | propene | $O_2$ | acrolein | pro-panal | aceton | CO | acitic acid | by-product | visible peak position (nm) | band gap energy (eV) |
| 617 | 3 | 12 | 28 | 16 | 7 | 39 | 9 | 1 | 722 | 1.96 |
| 673 | 4 | 12 | 30 | 17 | 3 | 34 | 9 | 7 | -- | -- |
| 723 | 8 | 18 | 42 | 10 | 4 | 31 | 7 | 6 | -- | -- |

arge broadening and significant overlap of the bands. The identification of the absorption bands is also rendered more difficult because the signal/noise ratio drops with increasing temperature. If the required temperature is relatively high under stoichiometric and catalytic conditions, the broadening and overlap of the bands can also be increased by deposits and redox processes.

In the case of propene oxidation the determination of the desired quantities from the spectroscopic feature is impeded by the following circumstances: On the one hand, the reaction must be carried out at temperatures of at least 513 K for HPA and 613 K for $Cs_2A$ in order to achieve an appreciable conversion. On the other hand, structural and electronic changes of the catalysts accompanied, for instance, by an enormous increase in the apparent absorption, already appear at low temperatures owing to the crystal water loss, which leads to the formation of iso-propanol. Consequently, a correlation between the spectroscopic and analytic data could not be found. From this one can conclude that for a possible correlation between the electronic structure of the working catalyst and its performance, the optimal catalyst temperature should be T < 623 K for a clear observation of the spectroscopic characteristics. For this reason reactants that are not reduced too strongly by the suitable working catalysts under catalytic conditions are necessary for the investigation of the redox states.

## Acknowledgments

The work was supported financially by the BMBF through its catalysis program (BMBF-Vorhaben 03D0058B). The authors are indebted to O. Timpe for preparing the heteropoly compounds and to M. Thiede for experimental assistance in UV/Vis/near-IR spectroscopy. One of the authors (S.Klokishner) is grateful to the Max-Planck-Gesellschaft for the visiting research grant.

## References

1. M. Misono, N. Nojiri, Appl. Catal., 1990, 64 ,1.
2. Th. Ilkenhans, B. Herzog, Th. Braun and R. Schlögl, J. Catal., 1995, 153 , 275.
3. L. Weismantel, J. Stöckel and G. Emig, Appl. Catal., 1996, 137 , 129.
4. B.B. Bardin and R.J. Davis, Appl. Catal. A, 1999, 185, 283.
5. T. Ilkenhans, PhD. thesis, Johann Wolfgang Goethe-Universität Frankfurt/M., 1996.
6. C. Rocchiccioli-Deltcheff and M. Fournier, J. Chem. Soc. Farad. Trans.,1991, 87 (24) , 3913.
7. B.W.L. Southward, J.S. Vaughan and C.T. O´Connor, J. Catal.,1995,153, 292.
8. G. Mestl, T.K.K. Srinivasan and H. Knözinger, Langmuir, 1995, 11, 3795.
9. L. Weismantel, J. Stöckel and G. Emig, Appl. Catal., 1996, 137 ,129.
10. J.K. Lee, V. Russo, J. Melsheimer, K. Köhler and R. Schlögl, Phys. Chem. Chem. Phys., 2000, 2, 2977.
11. M.A. Banares, H. Hu and I.E. Wachs, J. Catal., 1995, 155, 249.
12. G. Mestl and T.K.K. Srinivasan, Catal. Rev.-Sci. Eng., 1998, 40, 451.

13. G. Mestl, T. Ilkenhans, D. Spielbauer, M. Dieterle, O. Timpe, J. Kröhnert, F. Jentoft, H. Knözinger and R. Schlögl, Appl. Catal. A, 2001, 210 , 13.
14. S. Berndt, PhD. thesis, Technical University Berlin, 1998.
15. S. Berndt, D. Herein, F. Zemlin, E. Beckmann, G. Weinberg, J. Schütze, G. Mestl, and R. Schlögl, Ber. Bunsenges. Phys. Chem.,1998, 102, 763.
16. J. Kröhnert, Diploma thesis, Technische Fachhochschule Berlin, 1999.
17. J.J. Altenau, M.T. Pope, R.A. Prados, and H. So, Inorganic Chemistry, 1975, 14, 417.
18. G. Centi, J. Lopez Nieto and C. Iapalucci, Appl. Catal. 1989, 46 , 197.
19. G. Centi, V. Lena, F. Trifiro, D. Ghoussoub, C.F. Aissi, M. Guelton and J.P. Bonnelle, J. Chem. Soc. Faraday Trans.1990, 86, 2775.
20. D. Casarini, G. Centi, P. Jiru, V. Lena and Z. Tvaruzkova, J. Catal. 1993, 143, 325.
21. N.N. Timofeeva, A.V. Demidov, A.A. Davydov, I.V. Kozhevnikov, J. Mol. Catal., 1993, 79 , 21.
22. J. Melsheimer, Sabri S. Mahmoud, G. Mestl and R. Schlögl, Catalysis Letters, 1999, 60 ,103.
23. J.K. Lee, J. Melsheimer, S. Berndt, G. Mestl, R. Schlögl and K. Köhler, Appl. Catal.A, 2001, 214 ,125.
24. M. Thiede and J. Melsheimer, Rev. Sci. Instrum. (accepted for publication).
25. S. Klokishner, J. Melsheimer, R. Ahmad, F. C. Jentoft, and R Schlögl, to be published.
26. M.N.Popova, E.P.Chukalina, B.Z.Malkin,S.K.Saikin,Phys.Rev.B, 2000, 61 7421.
27. M.Che, F.Bozon-Verduraz, in: Handbook of Heterogeneous Catalysis, v.2, p.641-671, ed. G.Ertl, H.Knözinger, J.Weitkamp (Wiley - VCH, 1997).
28. S. Klokishner, J. Melsheimer, R. Ahmad, F. C. Jentoft, G. Mestl and R. Schlögl, Spectrochimica Acta, Part A (accepted for publication).
29. J.J.BorrasAlmenar, J.M.Clemente, E.Coronado, B.S.Tsukerblat, Chem. Phys., 1995, 195, 1.
30. C.Sanchez, J.Livage, J.P.Launay, M.Fournier,Y.Jeanin, J.Am.Chem. Soc., 1982, 104 , 3194.
31. B.B. Bardin, S.V. Bordawekar, N. Neurock, R.J. Davis, J. Phys. Chem., 1998, 102, 10817.
32. H. Taneta, S. Katsuki, K. Eguchi, T. Seiyama, N. Yamazol, J. Phys. Chem., 1986, 90, 2959.
33. D.Herein, O.Timpe, S.Berndt and G.Mestl, to be published.
34. C.J. Ballhausen and H.B. Gray, Inorganic Chemistry, 1962, 1, 113.